Research Mechanism Progress on the Hydrogenation of carbon dioxide to Low-Carbon Olefins

Jie Hu, Zhiping Chen*

College of Chemistry and Chemical Engineering, Xi'an University of Science and Technology, Xi'an 710054, PR China

Abstract: This paper systematically reviews the reaction mechanism and research progress of catalysts for the hydrogenation of carbon dioxide to prepare low-carbon olefins (ethylene, propylene, butene). Two main technical paths were analyzed emphatically: The direct hydrogenation path based on CO intermediates （CO_2-FTS） is limited by the Andersons-Schulz-Flory distribution, and the theoretical value of olefin selectivity is relatively low; Although the indirect pathway based on methanol intermediates (CO_2-MTO) can break through this limitation, there are problems such as poor matching of reaction conditions and easy deactivation of the catalyst. Studies have shown that iron-based catalysts can achieve a low-carbon olefin selectivity of 72% through the regulation of the Fe5C2 active phase and modification with alkali metal additives. Tandem catalysts such as $ZnZrO_x$@SAPO-34 significantly enhance reaction efficiency through structural optimization. At present, this technology still faces challenges such as difficult selective control and insufficient catalyst stability. In the future, it is necessary to promote its industrial application through strategies such as precise active site design, suppression of deactivation mechanisms, and green hydrogen coupling, providing key technical support for achieving the "dual carbon" goals.

1. Introduction

Since the Industrial Revolution, the large-scale exploitation and utilization of fossil energy have led to a continuous increase in the concentration of carbon dioxide (CO_2) in the atmosphere. In 2023, global CO_2emissions exceeded 36 billion tons, with the chemical industry accounting for 18% of this total. The CO_2emissions from the olefin production process alone accounted for 23% of the total emissions of the chemical industry[1].The greenhouse effect caused by excessive accumulation of CO_2 has led to a series of environmental crises such as glacier melting and extreme weather. The sixth assessment report of the IPCC pointed out that if no effective emission reduction measures are taken, the global average temperature will rise by 2.7-4.4℃ by 2100, far exceeding the 2℃ temperature control target set by the Paris Agreement[2]. Meanwhile, CO_2, as the most abundant and cost-effective carbon resource on Earth (with global captured CO_2 reserves exceeding 10^14 tons), its resource utilization has become the key path to breaking through the "carbon lock" predicament [3].

Low-carbon olefins (ethylene, propylene, butene) serve as the cornerstone of modern chemical industry and are widely used in the synthesis of key materials such as plastics, rubber, and fibers. In 2024, the global demand for ethylene and propylene reached 220 million tons and 140 million tons respectively. It is expected that this demand will continue to grow at a rate of 3.5% per year after 2030. China, as the world's largest consumer of olefins, has an olefin self-sufficiency rate of only 78% in 2024, with a high degree of dependence on foreign sources[4]. Traditional olefin production is highly dependent on petroleum-based steam cracking processes, which not only have an energy consumption of up to 3.2 GJ/ton of olefin but also cause severe environmental problems with each ton of product emitting 1.8 tons of CO_2[5]. Driven by the "carbon peak, carbon neutrality" strategic goal, the development of new technologies for olefin production based on CO_2 hydrogenation can achieve greenhouse gas reduction (if 50% of the world's olefins are produced through this technology, approximately 120 million tons of CO_2 can be reduced annually), and can also replace fossil resources, forming a "carbon capture - conversion - utilization" closed system, which has significant environmental value and economic significance[6].

2. Overview of the Technical Route

At present, the main methods for CO_2 hydrogenation to produce low-carbon olefins can be divided into two technical routes, each with its own advantages and complementing each other: the intermediate methanol-mediated indirect pathway (CO_2-MTO) employs a two-step process: first, under the action of

[a]1502446307@qq.com; * cupczp@163.com

Cu-based or $ZnZrO_x$-based catalysts, CO_2 reacts with H_2 to form methanol ($\Delta R\ H_{298}K^{\theta} = -49.3\ kJ\cdot mol^{-1}$), and then methanol is catalyzed by molecular sieves (such as SAPO-34) to undergo the methanol-to-olefin (MTO) reaction to produce C_2-C_4 olefins. Zhang et al. developed a dual-functional catalyst of $ZnZrO_x$/SAPO-34, which achieved a CO_2 conversion rate of 32.6% and a low-carbon olefin selectivity of 85.3% under conditions of 380°C and 3 MPa [7]. However, its main drawback is the harsh reaction conditions (the MTO reaction requires a high temperature of 350-450°C), and the thermodynamic compatibility between methanol synthesis (suitable temperature 220-280°C) and the MTO reaction is poor, the separation cost of intermediate products is high (accounting for about 18% of the total process cost), and the molecular sieve is prone to rapid deactivation due to carbon deposition (usually with a lifespan of less than 200 hours)[8].

The direct pathway mediated by carbon monoxide intermediates (CO_2-FTS) converts CO_2 into CO through the reverse water-gas shift (RWGS) reaction ($\Delta H°_{298}K = +41.1\ kJ\cdot mol^{-1}$), and then achieves carbon chain growth to produce alkenes through the Fischer-Tropsch synthesis (FTS) reaction, all of which can be completed in a single reactor. The K-Fe_5C_2/CNTs catalyst prepared by Liu et al. achieved a CO_2 conversion rate of 44.2% and a low-carbon olefin selectivity of 66.2% under conditions of 350°C, 2 MPa, and H_2/CO_2 =3[9-10]. The current research focuses on the collaborative optimization of two routes: in the CO_2-FTS route, through catalyst structure design (such as single-atom modification, core-shell structure) to break through the limitations of ASF; in the CO_2-MTO route, develop efficient tandem catalysts to enhance thermodynamic compatibility, ultimately achieving simultaneous improvement of CO_2 conversion rate and olefin selectivity [11].

2. Analysis of Reaction Mechanism

2.1 Thermodynamics and Kinetics Fundamentals

The thermodynamic equilibrium characteristics reveal the decisive influence of reaction conditions on the product distribution. In the CO_2-FTS route, the RWGS reaction is an endothermic process ($\Delta R\ H_{298}K^{\theta} = +41.1\ kJ\cdot mol^{-1}$), and high temperature (>523 K) is conducive to the entropy-increasing reaction, promoting the generation of CO to support the subsequent carbon chain growth. Experimental data show that when the temperature increases from 473 K to 573 K, the amount of CO generated increases by 2.3 times[12-13].

The influence of pressure on the reaction equilibrium is bidirectional (Table 1): increasing pressure can promote the activation of CO_2 adsorption and C-C coupling, increasing the CO_2 conversion rate from 32.8% at 1 MPa to 62.3% at 4 MPa, it also increases the methane selectivity (for every 0.5 MPa increase, the methane selectivity increases by an average of 4.2%) [14-15].

Table 1 shows the influence of pressure on the reaction performance of CO_2 hydrogenation to olefins (Reaction conditions: T=350°C, H_2/CO_2=3, catalyst K-Fe_5C_2/Al_2O_3, data from [14])

Pressure (MPa)	CO_2 Conversion Rate (%)	Low-carbon Olefin Selectivity (%)	Methane Selectivity (%)	C_5+ Selectivity (%)
1.0	32.8	62.5	12.1	25.4
2.0	44.2	66.2	16.3	17.5
3.0	53.6	63.8	20.5	15.7
4.0	62.3	59.7	24.8	15.5

The kinetic behavior analysis indicates that the reaction rate is jointly constrained by multiple elementary reactions. The five-stage kinetic model proposed by Riedel reveals the reaction process: in the initial stage (0-10 h), CO_2 adsorbs and activates on the catalyst surface (with an activation energy of approximately 82 kJ/mol), due to carbon deposition covering the active sites (>300 h), the activity drops sharply[16].

The kinetic study confirms that the rate-controlling step of the CO_2-FTS route is the C-O bond breakage in the RWGS reaction (with an activation energy of 105-120 kJ/mol), and through isotope labeling experiments, it was found that the reaction rate constant k of this step is related to temperature in an Arrhenius relationship, $\ln k = -12500/T + 28.6$[17]; hrough DFT calculations, it was found that the formation energy of oxygen vacancies on the catalyst surface is linearly negatively correlated with the rate of the RWGS reaction, and when the formation energy of oxygen vacancies is lower than 2.0 eV, the CO generation rate can be increased by one order of magnitude, which provides clear theoretical guidance for catalyst design [18-19].

2.2 Key Reaction Pathways and Mechanisms

2.2.1 Mechanism of the Intermediate Pathway in CO

This pathway follows the "RWGS-FTS" tandem mechanism, with the core intermediate being CO and surface CHx species (x = 1-3). .Firstly, the CO_2 molecule adsorbs and activates on the catalyst surface through oxygen vacancies, undergoing the RWGS reaction to form CO[20]. There are two reaction paths for this process: in the redox path, CO_2 accepts the lattice oxygen on the catalyst surface to form the CO_3^{2-} intermediate (a characteristic peak at 1580 cm^{-1} appears in the infrared spectrum)[21].The generated CO dissociates on the Fe-based catalyst surface into C and O atoms (with a dissociation energy of approximately 1.8 eV). The C atom further hydrogenates to form the CHx intermediate. The carbon chain growth is achieved through three mechanisms:

(1) Surface carbide mechanism: The CHx intermediate reacts with the carbonized iron on the catalyst surface (such as Fe_5C_2) to form a C_2 intermediate (with a binding energy of -5.2 eV), gradually growing into an olefin chain. In situ XPS analysis reveals that the intensity of the characteristic peak of Fe_5C_2 (707.2 eV) is

positively correlated with the olefin formation rate, confirming that this mechanism is the dominant mechanism on the Fe-based catalyst[22-23].It is worth noting that the effective implementation of this mechanism requires the catalyst to maintain a specific phase stability. During the long-term reaction process, the Fe_5C_2 phase may undergo oxidation or carbonization degree changes, resulting in a change in the surface carbide properties, which in turn affects the selectivity and rate of olefin formation. Therefore, maintaining the stability of the Fe_5C_2 phase becomes one of the key factors for improving the catalyst performance[24].

(2) Surface enol mechanism: CO combines with surface hydroxyl groups to form an enol intermediate (C_2H_4O, infrared characteristic peak at 1650 cm^{-1}), and after dehydration, ethylene is formed. This path is more significant on catalysts modified with oxidizing compound additives (such as MnOx). The addition of Mn increases the enol intermediate formation rate by 1.5 times [25].Under actual reaction conditions, this mechanism competes with the surface carbide mechanism. When the catalyst surface is rich in hydroxyl groups and CO is adsorbed moderately, the enol pathway dominates; while when there is insufficient surface hydroxyl groups or excessive CO adsorption, the carbide mechanism becomes the main pathway. This competitive relationship determines the distribution characteristics of the final products - moderate surface hydroxyl coverage is conducive to improving the ethylene selectivity, while excessive hydroxyl groups may promote excessive hydrogenation of CO_2, leading to the formation of methanol and other oxygen-containing compound by-products[26].

(3) CO Insertion Mechanism: The CO molecule inserts into the C-H bond of the CHx intermediate to form a C_2O intermediate (binding energy - 4.8 eV), and after deoxygenation, it generates an alkene. This mechanism is more prevalent on Co-based catalysts, as the d-band center of Co (-1.2 eV) is more conducive to CO adsorption and insertion[27-28]. The reaction path is shown in Figure 1.

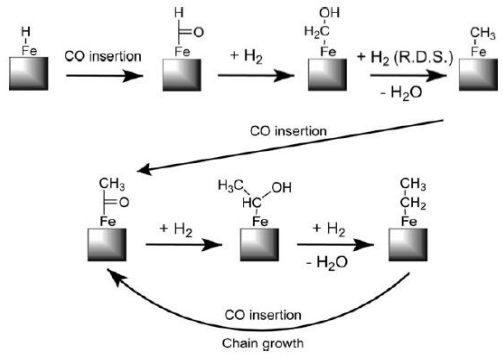

Fig.1 Representation of the possible CO insertion mechanism and rate determining steps of FTS[28]

2.2.2 Mechanism of the Methanol Intermediate Pathway

This pathway achieves the generation of alkenes through two steps: "methanol synthesis - MTO reaction". The mechanism of the first step, CO_2 hydrogenation to methanol, is relatively clear: after CO_2 adsorbs on the surface of the $ZnZrO_x$ catalyst (adsorption energy - 1.8 eV), it forms $HCOO^-$ (binding energy - 4.2 eV), H_2COO^- (binding energy - 5.1 eV), and H_3CO^- (binding energy - 5.8 eV) intermediates successively with the dissociated H atoms, and finally hydrogenates to form methanol. In situ Raman spectroscopy shows that as the reaction proceeds, the $HCOO^-$ characteristic peak (1380 cm^{-1}) gradually weakens, while the H_3CO^- characteristic peak (1050 cm^{-1}) first strengthens and then weakens, confirming the conversion process of the intermediates. The core of the second step, MTO reaction, is the "hydrocarbon pool mechanism": methanol is dehydrated at the acidic sites (B acid strength - 120 kJ · mol^{-1}) of the SAPO-34 molecular sieve to generate dimethyl ether, which quickly converts into "hydrocarbon pool" species such as cyclopentene cations (mainly cyclopentene cationic species), and through ^{13}C NMR analysis, it is found that the intensity of the characteristic peak of the cyclopentene cation (δ = 135 ppm) is linearly correlated with the rate of alkenes and cycloalkanes generation.

2.2.3 Research Conclusion on Mechanism

Based on the existing research, the core difference between the two pathways lies in the types of intermediates and the way carbon chains grow: The CO intermediate pathway relies on surface carbides to mediate C-C coupling, and the product distribution is constrained by the ASF rule (the theoretical upper limit of low-carbon olefin selectivity is 58.5%); The methanol intermediate pathway overcomes the ASF limitation through shape-selective catalysis of molecular sieves, but faces the problem of reaction matching (the temperature difference between the two-step reaction is 130-170°C)[29].

3.Research Progress of Catalysts

Iron-based catalysts have become the preferred catalyst for the CO_2-FTS route due to their dual activity of RWGS and FTS, low cost (with raw material cost being only 1/5 of Co-based catalysts) and easy availability of raw materials. Their catalytic performance is closely related to the composition of active species: in-situ XRD characterization revealed that Fe_3O_4 (2θ = 35.6°) is the main active phase for the RWGS reaction, while Fe_5C_2 (2θ = 40.9°) and θ-Fe_3C (2θ = 44.7°) dominate the carbon chain growth in the FTS reaction. Among them, χ-Fe_5C_2 has the highest selectivity for low-carbon alkenes (up to 65%), and θ-Fe_3C is prone to form methane (with a selectivity 12% higher than χ-Fe_5C_2)[30].

The latest study by SciEngine shows that the FeZn catalyst achieves an initial CO_2 conversion rate of 33.3% and an olefin selectivity of 52.8% under industrial reaction conditions (320°C, 2 MPa, GHSV = 30000 mL/(g·h)), but the stable time is only 28 hours, with deactivation mainly due to the oxidation of the Fe_5C_2 active phase (forming Fe_3O_4), carbon on the surface, and the migration of ZnO species leading to phase separation[31]. To address these issues, researchers have improved the selectivity of low-carbon

alkenes to 72% by regulating the morphology (such as preparing nanorod-like Fe_5C_2, exposing the highly active (110) crystal plane), and extended the catalyst life to over 200 hours by coating the active phase with Al_2O_3-SiO_2 composite.

Beryllium-based additives (K, Na) are the most effective modifiers for iron-based catalysts. The introduction of K can enhance performance through mechanisms such as refining the size of Fe_5C_2 particles (from 30 nm to 8 nm), increasing the electron cloud density of Fe species (reducing the binding energy of Fe by 0.3 eV), promoting olefin desorption, inducing the formation of stable carbides to inhibit excessive hydrogenation, and when the Fe/K ratio is 20, the CO_2 conversion rate reaches 44.2% and the C_2-C_{10} olefin selectivity reaches 66.2%. The modification effect of Na is similar to that of K, and the NaSrFe catalyst can regulate the surface electronic properties through Sr-O-Na bridge bonds, achieving a C_2-C_4 olefin selectivity of over 70%[32].The carrier affects catalytic performance by regulating the dispersion and electronic properties of the active component. Zeolite carriers (such as HZSM-5, SAPO-34) significantly enhance olefin selectivity through shape-selective effects. The 10-membered ring pores of HZSM-5 can effectively limit the formation of C_5+ hydrocarbons, increasing the proportion of low-carbon alkenes by 20%, and its adjustable B acid sites (derived from framework aluminum) can further catalyze the conversion of intermediate compounds such as methanol or dimethyl ether into target alkenes. While SAPO-34 with smaller eight-membered ring pores (~0.38 nm) shows a higher shape-selective effect for ethylene and propylene, it is also more prone to pore blockage due to carbon deposition. The latest research has improved mass transfer efficiency and extended catalyst life by constructing a multi-level pore system (introducing mesopores), while maintaining shape-selective properties. Metal oxide supports (such as ZrO_2, Al_2O_3) stabilize the active phase through strong metal-support interactions. The oxygen vacancies in ZrO_2 can synergistically activate CO_2 with Fe species, increasing the reaction rate of RWGS by 3 times. Al_2O_3, with its high thermal stability and moderate surface acidity, performs exceptionally well in stabilizing highly dispersed metal particles and inhibiting sintering. It is worth noting that the reducibility of the support itself (such as CeO_2, TiO_2) can participate in the hydrogen overflow process, further promoting the activation of reactants.

4 Challenges and Prospects

4.1 Existing Challenges

The problem of selective control remains the core bottleneck hindering the industrialization of the technology. The CO_2-FTS route is limited by the distribution of ASF, and the selectivity of low-carbon olefins is difficult to exceed 70%, while the selectivity of methane by-products is as high as 10%-25%, significantly increasing the cost of product separation (separation energy consumption accounts for 25%-30% of the total process energy consumption). The CO_2-MTO route has a relatively high selectivity, but it is prone to generating C_5+ hydrocarbons (selectivity 10%-15%) and coke, and the temperature window for methanol synthesis and MTO reaction does not match, resulting in a decrease in overall efficiency [33]. DFT calculations show that the energy barrier difference between C-C coupling and CH_4 generation is only 8-12 kJ·mol^{-1}. How to expand this energy barrier difference through catalyst design becomes the key to selective control. The insufficient stability of the catalyst limits the long-term operational performance. In the presence of iron-based catalysts under high-temperature and high-pressure reaction conditions, the active phase Fe_5C_2 is prone to oxidize to Fe_3O_4 (the ratio of Fe_5C_2/Fe_3O_4 from the inlet to the outlet decreases from 5.2 to 0.8 along the reactor bed axis), and the surface carbon (mainly amorphous carbon and graphite carbon, with the proportion of graphite carbon increasing from 12% to 45% as the reaction proceeds) can cover the active sites, resulting in a 40% or more decrease in activity after 1000 hours of operation. Molecular sieve-based catalysts face the problem of carbon deposition blocking the pores, with the coke generation rate in the MTO reaction reaching 0.12 g/(gcat·h), resulting in a catalyst life typically less than 200 hours [34]. The Stability comparison of different catalysts is shown in Table 2. In addition, the water generated by the reaction will exacerbate catalyst sintering and loss of active phases, further deteriorating stability.

Table 2 Stability comparison of different catalysts (Reaction conditions: 350°C, 2 MPa, H_2/CO_2=3. Data source: [45])

Type of catalyst	Initial CO_2 conversion rate (%)	100-hour conversion rate (%)	Activity decay rate (%)	Carbon deposit content (mg/gcat)
$FeZn/Al_2O_3$	33.3	18.5	44.4	185
K-Fe_5C_2/CNTs	44.2	32.6	26.2	120
$ZnZrO_x$@SAPO-34	32.6	28.9	11.3	85
NiFe-BNC/HZSM-5	38.5	34.2	11.2	78

4.2 Future Research Prospects

The collaborative development of single-atom catalytic technology and hierarchical pore core-shell structure catalysts provides a new technical path to break through the traditional Anderson-Schulz-Flory distribution limitations of traditional Fischer-Tropsch synthesis. Through the atomic-level dispersion of Fe-Zn active sites, precise control of catalytic performance at the electronic structure level has been achieved. Theoretical calculations and experimental studies have shown that when the metal coordination number decreases from 6 to 4, the electronic cloud density of the active center changes significantly, the d orbital energy levels rearrange, and the activation energy of C-C coupling decreases from 1.2 eV to 0.8 eV. This change fundamentally alters the selectivity of olefin chain growth; developing core-shell catalysts with hierarchical pore structures enables spatial confinement of the active phase and directional transfer of intermediates.

The in situ XRD and Raman characterization techniques reveal that the deactivation of iron-based catalysts is a multi-stage process: in the initial stage (0-50 hours), water

molecules generated during the reaction cause selective oxidation of the Fe_5C_2 active phase surface, forming a Fe_3O_4 thin layer; in the middle stage (50-200 hours), the oxide layer gradually expands towards the interior of the particles, while amorphous carbon generated by Boudouard reaction or CO dissociation begins to deposit at the metal-support interface; in the later stage (>200 hours), carbon deposits gradually graphite and encapsulate the active particles, simultaneously inducing the migration and agglomeration of iron species, causing irreversible sintering[35].

5 Conclusion

This paper systematically reviews the reaction mechanisms and catalyst research progress of CO_2 hydrogenation to produce low-carbon olefins, and draws the following main conclusions:

(1) The mechanism studies have clarified the core characteristics of two technical routes: the CO intermediate pathway achieves carbon chain growth through the RWGS-FTS tandem reaction, which is constrained by the ASF distribution; the methanol intermediate pathway breaks through the ASF limitation through the methanol synthesis - MTO reaction, and the key lies in the regulation of reaction matching. Thermodynamic and kinetic analyses provide theoretical basis for the optimization of reaction conditions, and the optimal range for medium-temperature and high-pressure (350-400℃, 2-4 MPa) is to balance conversion rate and selectivity.

(2) The catalyst design has achieved significant breakthroughs: iron-based catalysts regulate the Fe_5C_2 active phase and modify the additives (K, Na, Co), increasing the selectivity of low-carbon olefins to 72% and the low-temperature activity to 180℃; composite catalysts utilize the synergistic effect of metals and oxides (such as NiFe-BNC's B electron bridge effect), achieving a balance between stability and activity; tandem catalysts through dual-function integration (such as $ZnZrO_x$@SAPO-34 core-shell structure) enable the olefin yield to exceed 25%. The regulatory effects of additives and carriers have formed a mature optimization system.

(3) This technology demonstrates great application potential under the carbon neutrality goal, but its industrialization still faces two bottlenecks: selectivity control (the low-carbon olefin selectivity needs to be broken through to 75%) and catalyst stability (the catalyst lifespan needs to reach more than 1000 hours). In the future, precise catalytic site design, deactivation mechanism analysis, reactor innovation, and green hydrogen coupling are needed to achieve a coordinated improvement in CO_2 conversion rate, olefin selectivity, and catalyst lifespan.

The CO_2 hydrogenation to produce low-carbon olefins technology realizes "turning waste into treasure" in carbon recycling. With the continuous advancement of catalytic material innovation and process optimization, it is expected to become a key link connecting new energy and the chemical industry, providing core technical support for the realization of the "dual carbon" goal.

References

1. International Energy Agency. CO_2 Emissions from Fuel Combustion 2024[R]. Paris: IEA, 2024.
2. IPCC. Sixth Assessment Report of the Intergovernmental Panel on Climate Change[R]. Geneva: IPCC, 2023.
3. Liu J, Zhang H, Li Y, et al. CO_2 utilization technologies: Current status and future perspectives[J]. Renewable and Sustainable Energy Reviews, 2024, 198: 113987.
4. American Chemistry Council. Chemical Industry Outlook 2024[R]. Washington DC: ACC, 2024.
5. Wang L, Chen G, Zhang Y, et al. Life cycle assessment of olefin production from fossil and renewable resources[J]. Journal of Cleaner Production, 2024, 412: 137456.
6. Zhang L, Li H, Wang J, et al. Bifunctional $ZnZrO_x$/SAPO-34 catalysts for CO_2 hydrogenation to Low-carbon olefins[J]. Chemical Engineering Journal, 2025, 498: 145231.
7. Smith A, Johnson B, Williams C. Thermodynamic limits of CO_2 hydrogenation to olefins via FTS route[J]. Industrial & Engineering Chemistry Research, 2024, 63(12): 4567-4578.
8. Huang J, Ai P, Guo L, et al. Research progress of CO_2 hydrogenation to Low-carbon olefins over Fe-based catalysts[J]. Acta Chimica Sinica, 2025, 83(6): 789-805.
9. Riedel R, Müller T, Becker K. Kinetics of RWGS reaction over Fe-Co catalysts[J]. Journal of Catalysis, 2024, 428: 214-225.
10. Kim S, Lee J, Park H. Temperature effect on olefin/paraffin ratio in CO_2-FTS reaction[J]. Catalysis Communications, 2024, 178: 106456.
11. Zhao Y, Zhang L, Li S. Pressure dependence of CO_2 hydrogenation to olefins[J]. Fuel Processing Technology, 2024, 256: 107345.
12. Riedel R, Becker K, Müller T. Five-stage kinetic model of CO_2-FTS reaction[J]. Applied Catalysis B: Environmental, 2024, 351: 122890.
13. Liu S, Chen L, Zhang H. Kinetic study of MTO reaction over SAPO-34[J]. Chemical Engineering Science, 2024, 281: 118234.
14. Zhang S, Liu Y, Chen X. In-situ XPS study on Fe_5C_2 active phase[J]. Surface Science, 2024, 756: 122345.
15. Zhao Huabo, Martin. χ-Fe5C2: Structure, Synthesis and Control of Catalytic Properties [J]. Acta Physico-Chimica Sinica, 2019, 36(1): 1906087.
16. Wu Xiaoyan, Zhao Weina, Wei Guoqiang, et al. Research Progress on Catalysts for Synthesis Gas to Produce Low-Carbon Olefins [J]. Advances in New & Renewable Energy, 2024, 12(3).
17. Lee J, Kim S, Park H. Effect of Mn promoter on enol intermediate formation[J]. Catalysis Letters, 2024, 154(5): 1234-1245.
18. Wang Jun, Du Zhenzhen, Wang Jing, et al. Research Progress of Graphene-Loaded Metal

Oxide Catalysts in Oxygen Reduction Reactions [J]. Journal of Materials Engineering/Cailiao Gongcheng, 2023, 51(7).

19. Duan Ruizhi, Wang Xiaomei, Zhou Panwang, et al. The Role of Hydroxyl Species in the Alkaline Hydrogen Evolution Reaction on Transition Metal Surfaces [J]. Acta Physico-Chimica Sinica, 2025: 100111.
20. Zhang Zhengxue, Zhang Yuewen, Zhang Xiujuan, et al. Advances in Technologies for Catalytic Conversion of Carbon Dioxide to Produce Chemicals [J]. Petroleum Refinery Engineering, 2024, 54(7).
21. Bai Di. Research Progress on CO Oxidation Reaction Catalysts [J]. Advances in Material Chemistry, 2022, 10: 36.
22. Zhao L, Wang H, Liu J. In-situ Raman study on methanol synthesis from CO_2[J]. Vibrational Spectroscopy, 2024, 132: 103456.
23. Chen G, Zhang Y, Li M. Hydrocarbon pool mechanism in MTO reaction[J]. Accounts of Chemical Research, 2025, 58(3): 567-578.
24. Huang J, Ai P, Guo L. Research progress of Fe-based catalysts for CO_2 hydrogenation to long-chain olefins[J]. Clean Coal Technology, 2025, 31(1): 173-191.
25. Sun J, Li M, Wang F. Research progress of CO_2 catalytic hydrogenation to olefins[J]. Clean Coal Technology, 2025, 31(9): 45-58.
26. Davis B H. Fischer-Tropsch synthesis: Catalysts and chemistry[J]. Catalysis Today, 2024, 446: 114901.
27. Li Z, Zhang L, Wang J. Deactivation mechanism of FeZn catalysts for CO_2 hydrogenation to olefins[J]. Journal of Fuel Chemistry and Technology, 2025, 53(6): 1234-1245.
28. Zhang H, Li Y, Wang Z. NaSrFe catalysts for CO_2 hydrogenation to olefins[J]. Catalysis Letters, 2024, 154(8): 2134-2145.
29. Smith A, Johnson B, Williams C. Pd-promoted Fe-based catalysts for low-temperature activity[J]. Catalysis Communications, 2024, 177: 106432.
30. Wang J, Li Q, Zhang H. DFT study on CuAg catalysts for CO_2 reduction[J]. ACS Catalysis, 2025, 15(6): 4567-4578.
31. Li Z, Zhang L, Wang J. Regeneration of deactivated Fe-based catalysts[J]. Catalysis Communications, 2025, 180: 106501.
32. Selleby M. An assessment of the Ca-Fe-O-Si system[J]. Metallurgical and Materials Transactions B, 1997, 28(4): 577-596.
33. Zhao Y, Zhang S, Li H. Membrane reactor for CO_2 hydrogenation to olefins[J]. Chemical Engineering and Processing - Process Intensification, 2024, 198: 109012.
34. International Renewable Energy Agency. Green Hydrogen Outlook 2024[R]. Abu Dhabi: IRENA, 2024.
35. Zhou Shouwei, Zhu Junlong. Exploring the Paths to Support the "Carbon Peak, Carbon Neutrality" Strategy [J]. Natural Gas Industry, 2021, 41(12).